Surface treatment of hematite photoanodes with zinc acetate for water oxidation

Xi, Lifei; Bassi, Prince Saurabh; Chiam, Sing Yang; Mak, Wai Fatt; Tran, Phong D.; Barber, James; Loo, Say Chye Joachim; Wong, Lydia Helena

2012

Xi, L., Bassi, P. S., Chiam, S. Y., Mak, W. F., Tran, P. D., Barber, J., et al. (2012). Surface treatment of hematite photoanodes with zinc acetate for water oxidation. Nanoscale, 4(15), 4430-4433.

https://hdl.handle.net/10356/94963

https://doi.org/10.1039/C2NR30862B

Nanoscale

Cite this: DOI: 10.1039/c2nrxxxxxx

www.rsc.org/nanoscale

COMMUNICATION

Surface treatment of hematite photoanodes with zinc acetate for water oxidation

Lifei Xi [a], Prince Saurabh Bassi [a], Sing Yang Chia [b], Wai Fatt Mak [a], Phong D. Tran [c], James Barber [a,d,e], Joachim Say Chye Loo [*a], Lydia Helena Wong [*a]

Received (in XXX, XXX) Xth XXXXXXXXX 2012, Accepted Xth XXXXXXXXX 2012
DOI: 10.1039/c2ra00000x

A simple and inexpensive method to form a hematite photoanode for efficient water oxidation is reported. A very thin ZnO overlayer was deposited on top of a thin film of hematite and found, compared with non-treated hematite, to increase the photocurrent and reduce the onset potential for generating oxygen from water. After 3 cycles of ZnAc treatment, the photocurrent increased more than 40% to 1.08 mA/cm^2 at 0.23 V vs Ag/AgCl and onset potential for water oxidation shifted by -170 mV. It is proposed the ZnO overlayer changes the flat band potential of hematite and reduces the surface defects.

In recent years, α-Fe_2O_3 (hematite) has received considerable attention as a photoanode capable of oxidizing water due to its favourable optical band gap for visible light absorption (E_g=2.2 eV), appropriate redox potential of its valency band, excellent chemical stability, high abundance, and low cost. [1] It has been theoretically predicted that a semiconductor with this band gap could achieve a water splitting efficiency of 16.8%. [2] However, the reported efficiencies of α-Fe_2O_3 are notoriously lower than this predicted value, mainly due to the short photo-generated charge carriers lifetime (<10 ps) and short hole diffusion length (2-4 nm). [3] Another fundamental limitation of pure Fe_2O_3 system is the need for externally applied bias because the conduction band of Fe_2O_3 is lower than the potential required to reduce protons to hydrogen (in the vacuum scale). Currently, a few strategies can be used to address these issues by controlling dimensions and morphology of hematite at the nanometer scale. These strategies include making porous thin films using solution-based colloidal methods, [4, 5] nanowire arrays on substrates using template or hydrothermal methods, [6] electrodeposition, [7] spray pyrolysis, [8] atomic layer deposition (ALD) [9] and atmospheric pressure chemical vapor deposition (APCVD).[10] However, even with these improvements, water oxidation efficiencies of the various hematite systems are still far below expectation, partly because of recombination events due to the presence of nanograins. Surface treatment was previously found to be an effective way to improve performance. The reported materials include CoF_3, [11] Ga_2O_3, [12] Al_2O_3, [13] Al^{3+} and Sn^{4+} ions. [14] Hu et al. found that the onset potential shift is close to 200 mV for Ti-doped hematite modified with CoF_3. [11] However, HF, one of the side products of the surface treatment, is highly corrosive and toxic. Le Formal et al [13] found a 100 mV shift of the onset potential when hematite was covered with Al_2O_3 deposited by atomic layer deposition (ALD). These studies have shown that surface treatment of hematite photoanodes not only reduces the overpotential but also facilitates interfacial electron transfer, thus increasing the photocurrent for photoelectrochemical (PEC) cells. Clearly, surface treatment of photoanodes using safe, inexpensive materials and simple processing techniques to develop high performance devices is of considerable interest.

This study reports for the first time an inexpensive spin coating method for the deposition of ZnO onto a thin film of hematite from a solution of ZnAc. As compared to ALD, that is expensive and requires high vacuum, the spin coating method employed here is simpler, cheaper and can be used to deposit a wider selection of materials. ZnO is a wide bandgap semiconductor of the II-VI group that has several favourable properties: inexpensive, good transparency, high electron mobility with reduced recombination loss and environmental compatibility. [15-16] Its bandgap is 3.3 eV at room temperature and is already being explored for use in transparent electrodes in liquid crystal displays, electronics applications for thin film transistors, light-emitting diodes and solar cells. [17] It is selected as the passivation layer because of good transparency, good transport properties, easy processing and high electrochemical stability. [16] On top of that, Fan et al. found that at low temperature (350°C), Zn introduced onto the surface of the Fe_2O_3 nanobelts serves as an electron donor thus contributing to enhanced n-type conductivity (almost four orders of magnitude increased). [18] This is because Zn has a smaller atomic radius (R_{zn} =0.142 nm) than that of Fe (R_{Fe}=0.156 nm). They also found Zn doping can modify the band edge of Fe_2O_3 nanobelts. These properties and phenomenon motivated us to modify Fe_2O_3 film with ZnAc and this study is of particular importance for surface modification of Fe_2O_3 when pursuing a good balance between of stability, performance, safety and ease of production.

In this study, we show that the onset potential for hematite driven water oxidation improved by 170 mV after ZnAc treatment. We also show that three cycles of ZnAc treatment can enhance the photocurrent from 0.75 to 1.08 mA/cm^2 at 0.23V *vs* Ag/AgCl under standard AM1.5 sunlight conditions, representing a maximum improvement of 40% compared with untreated α-

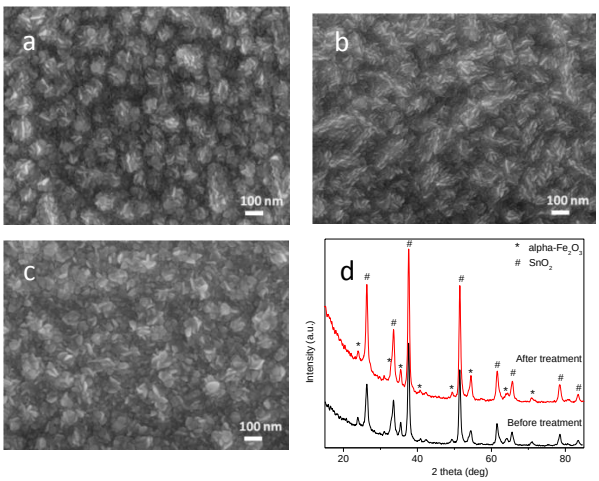

Fig. 1 SEM images of hematite films (a) before, (b) after ZnAc treatment and (c) after 3hr of PEC test. (d) XRD pattern of hematite film before and after ZnAc treatment. The * denotes Fe2O3 (JCPDS 33-0664) and # denotes SnO2 (JCPDS 46-1088), respectively.

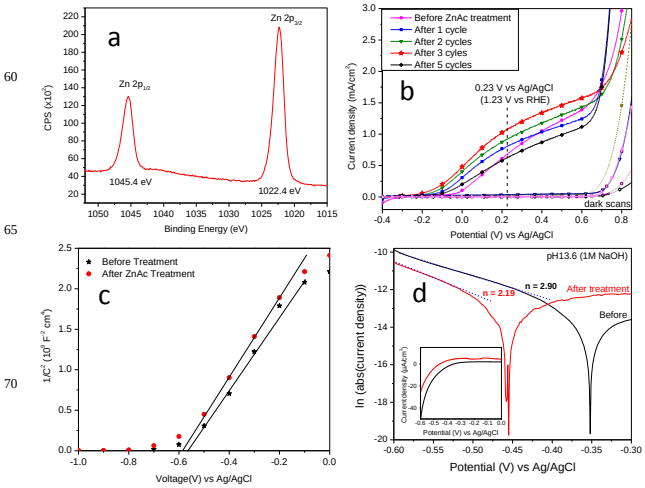

Fig. 2 (a) XPS spectra of hematite films after ZnAc treatment (Zn 2p scan). (b) Photocurrent-potential curves before and after different cycles of ZnAc treatment. (c) Mott-Schottky plots of hematite films in a 1 M NaOH electrolyte in the dark. (d) Local ideality factor extracted from the dark I-V curves (inset) before and after surface treatment.

Fe_2O_3. This improvement in the photocurrent is much higher than that reported by Hisatomi et al. [12] In that study, the photocurrent at 0.23 V *vs* Ag/AgCl was only increased from 0.37 to 0.42 mA/cm^2 (ca. 14%) after treated with Ga_2O_3. The pronounced effect of surface treatment with ZnAc is reproducible; in more than 10 photoanodes tested (with initial photocurrents of 0.5-0.8 mA/cm^2), the photocurrents have been enhanced to 20-40% after surface treatment. Although our maximum photocurrent is lower than that of doped hematite photoanodes prepared by APCVD, [10] it is still much higher than that of many reported un-doped hematite photoanodes prepared by spray pyrolysis methods. [19-22] For example, Le Formal et al. only obtained a maximum photocurrent of 0.42 mA/cm^2 at 0.23 V *vs* Ag/AgCl. [19] Zhang et al. obtained 0.93 mA/cm^2 at 0.23 V *vs* Ag/AgCl. [21] It was proposed that the very thin layer of ZnO modifies the flat band potential as well as reduce surface defects.

The hematite photoanodes used in this work were fabricated by spray pyrolysis (ESI†). Surface treatments of photoanodes were done by spin-coating 25 mM zinc acetate (ZnAc, 99%, Sigma) solution in ethanol. After that, the photoanodes were annealed at 400 °C for 20 min. A diagrammatic representation of the photoanode structure and SEM image of SnO_2 are shown in Fig. S1a-b (ESI†). It can be seen that a uniform compact layer is formed on top of FTO. It was found that the presence of this thin SnO_2 blocking layer can direct the growth of α-Fe_2O_3 in the [110] direction. [23] Liang et al. proposed that such unidirectional growth can improve band alignment between the Fe_2O_3 and the underlying FTO. [24] We propose that this thin layer of SnO_2 can also prevent charge recombination at the interface of FTO. In addition, Sn doping from this thin layer of SnO_2 may occur during annealing at 550°C for 2 hr. The SEM top view image of the sample before treatment with ZnAc revealed a mesoporous structure (Fig. 1a). It can be seen that there is a mixture of nanoplates and nanoneedles on the surface of hematite film. The size ranges from few tens to hundred nanometers. A mesoporous film is preferred because it increases the surface area, thus increasing the charge transportation to semiconductor/electrolyte interface. [1] SEM image after ZnAc treatment reveals a similar morphology (Fig. 1b). However, after 3 hr of PEC measurement under AM1.5 conditions, the morphology changed dramatically (Fig. 1c). The nanoneedles partially disappeared, while nanoplates became more dominating. This may be an indication that a slow corrosion of hematite occurs during PEC experiments in strong base conditions.

A thickness of 90 nm was reached after 70 ml solution was sprayed (Fig. S1c, ESI†). Further increase in the hematite thickness decreases device performance, which is a consequence of the short hole diffusion length of hematite, leading to recombination of photoexcited holes and electrons. [25] XRD patterns of the films before and after ZnAc treatment (Fig. 1d) exhibit the formation of hematite phase with preferred orientation in the [110] axis vertical to the substrate. This result indicates that the (001) plane is oriented vertically to the substrate. [3] Such an organisation is beneficial for photoanode activity because the conductivity in the basal plane (001) is up to 4 orders of magnitude higher than the orthogonal planes and this preferred orientation should facilitate charge transport and collection during the photo-oxidation process. The absence of additional peaks after 3 cycles of ZnAc treatment in XRD pattern indicates that the Zn-based overlayer is very thin. XPS spectra of hematite after surface treatment confirmed the presence of Zn and corresponded to oxidized Zn and not its metallic form, as plasmon peaks of metallic Zn was not observed in the spectra (Fig. 2a and Fig. S2, ESI†). The Zn signal at the surface is substantial and the thickness is estimated to be a few nanometers.

Photocurrent-potential curves of hematite films before and after different cycles of ZnAc treatment are shown in Fig. 2b and Fig. S3 (ESI†). It was found that the ZnAc treatment gave rise to a strong effect on the photocurrent-potential characteristics of the hematite photoanodes. The photocurrent density increases from 0.75 before treatment to 0.80, 0.92 and 1.08 mA/cm^2 after 1, 2 and 3 cycles of ZnAc treatment, respectively. It is worthy to note that the efficiency of solar water splitting in this study is equal to 1.08% (η = J (mA/cm^2) · (1.23 - E_{appl}) (V) / 100 (mW/cm^2) · 100%, [26] where J is the current density, E_{appl} is the applied bias,

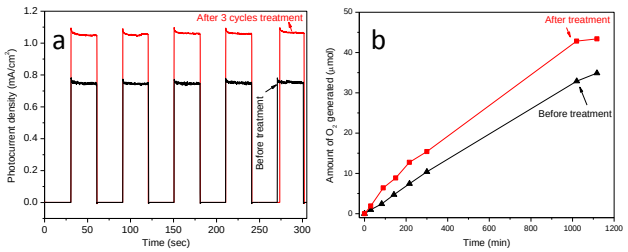

Fig. 3 (a) Photocurrent profile before and after 3 cycles of ZnAc treatment. (b) Time course of oxygen evolution of hematite films at an applied potential of 0.2 V vs Ag/AgCl in a 1 M NaOH electrolyte.

0.23 V is used in this calculation) which is still far below that of ideal semiconductor materials. [2] Further increasing ZnAc treatment to 5 cycles resulted in a decrease of photocurrent which is probably due to the formation of a thicker ZnO overlayer on top of hematite which may block the hole transport to the interface. The most likely reason for the increase in photocurrent after surface treatment with ZnAc is a decrease in the recombination reactions at the hematite/electrolyte interface. Recombination of photoexcited holes with electrons at the surface would be expected to be suppressed by the ZnO overlayer and thus facilitate the transport of photoexcited holes to the electrode/electrolyte interface. [12] Furthermore, this thin layer of ZnO may also act as an electron blocking layer to prevent electrons leaking from hematite into electrolyte. The photocurrent onset potential for the control sample is approximately -0.07 V *vs* Ag/AgCl whereas the values are about -0.14, -0.17 and -0.24 V *vs* Ag/AgCl after 1, 2 and 3 cycles of ZnAc treatment. The highest onset potential shift obtained after 3 cycles of surface treatment was around 170 mV. Increasing the surface treatment cycles to 5 resulted in the onset potential of around -0.1 V whereas the photocurrent decreased significantly.

In order to study the reason for onset potential shift, electrochemical impedance spectroscopy (EIS) measurements were carried out (Fig 2c). Mott-Schottky analysis at a frequency of 10 KHz showed the flat band potential of our untreated Fe_2O_3 photoanodes was around 0.578 V which is in line with previous reported values for Fe_2O_3 nanowires. [3] After ZnAc treatment there was an increase of approximately 39 mV in the magnitude of the negative flat band potential (V_{fb}). A 150mV shift has been recorded previously with CoF_3-treated hematite. [11] In our case, the negative V_{fb} shift after surface treatment is likely to be the result of electron donation from ZnO to the Fe_2O_3 interface which would be expected to shift the band edge to more negative value (Fig. S4, ESI†). This conclusion is consistent with that of Fan et al. [18] They proposed that Zn doping can modify the band edge of Fe_2O_3 nanobelts. Since the V_{fb} shift of ~ -39 mV only partially contributes to the total onset potential shift, the ZnO overlayer may also neutralize surface defects and therefore reduce recombination of charges. [12, 13] To confirm that the ZnO overlayer affects the recombination events, the ideality factor before and after surface treatment were extracted from dark I-V curves under forward bias (Fig. 2d and Fig. S5, ESI†). [27, 28] Ideality factor is calculated from the slope of the forward bias region of a *ln (I) vs* V plot. Since hematite is n-type semiconductor, the forward bias region of the I-V curve is at negative potential. [27] In this region, the recombination of charge carriers at the interface can be studied. The decrease of ideality factor after surface treatment is consistent with changes in recombination mechanisms. Therefore it seems that after surface treatment, the defects at the semiconductor surface were passivated, thus the chance of recombination at the interface of semiconductor/electrolyte was lowered.

In order to check whether the improvement of photocurrent could in part also be due to any change in optical absorption properties of the ZnAc treated samples, visible absoption spectra for treated and untreated samples were recorded (Fig. S6, ESI†). It can be seen that the shape of the absorption curves and the Tauc-Plots fitted bandgaps were nearly the same for both. Furthermore, the large bandgap of ZnO is not likely to be involved since a solar filter for blocking most UV light was employed when all PEC measurements were carried out. Fig 3a shows the photocurrent stability profile, which demonstrates that ZnAc treated system is as stable as the non-treated Fe_2O_3 photoanode under identical conditions (also refer to Fig. S7, ESI†). This was further confirmed by recording oxygen generation by gas chromatography. As shown in Fig 3b, the amount of oxygen generated after surface modification is stable and larger than that without treatment. Indeed, the stability of our modified photoanode is better than that of hematite modified with Al_2O_3 or CoF_3 (Fig. 3b). [11, 13] Hematite thin films covered with Al_2O_3 are stable for 30 min [13] while the stability of CoF_3 modified hematite is up to 50 min. [11]

In summary, we have demonstrated a safe, simple and inexpensive surface treatment of hematite that can increase the photocurrent and shift the onset potential to a more negative value for light-induced water oxidation. The onset potential of photoanodes was improved by 170 mV after 3 cycles of ZnAc treatment, while photocurrent was increased from 0.75 to 1.08 mA/cm^2 at 0.23V *vs* Ag/AgCl. The surface treatment of photoanodes resulted in the formation of an ultrathin layer of ZnO. It is proposed that the ZnO film acts as an electron blocking layer and reduces recombination of photoexcited holes and electrons at the surface, which together, leads to an increase in the performance of the system.

Acknowledgement

The funding from MOE ACRF Tier 1 and Centre of Artificial Photosynthesis is gratefully acknowledged.

Notes and references

[a] *School of Materials Science and Engineering, Nanyang Technology University, Singapore, 639798*
E-mail: Joachimloo@ntu.edu.sg, Lydiawong@ntu.edu.sg
[b] *Institute of Materials Research and Engineering(IMRE), Agency of Science, Technology, and Research (A* Star),3 Research Link, Singapore 117602, Singapore.*
[c] *Energy Research Institute @ NTU, Nanyang Technological University, 50 Nanyang Drive, Research Techno Plaza, X-Frontier Block, Level 5, Singapore 637553*
[d] *Division of Molecular Biosciences Imperial College London, London, SW7 2AZ, UK*
[e] *BioSolar Laboratory, Department of Material Sciences and Chemical Engineering, Polytechnic of Torino, Corso Duca degli Abruzzi, 24, 10129, Torino, Italy*

† Electronic Supplementary Information (ESI) available: Experimental details, characterizations and supporting figures. See DOI: 10.1039/b000000x/

1 K. Sivula, F. Le Formal and M. Gratzel, *ChemsusChem*, 2011, **4**, 432.

2 A. B. Murphy, P. R. F. Barnes, L. K. Randeniya, I. C. Plumb, I. E. Grey, M. D. Horne and J. A. Glasscock, *Int. J. Hydrogen Energy*, 2006, **31**, 1999.

3 Y. Ling, G. Wang, D. A. Wheeler, J. Z. Zhang and Y. Li, *Nano Lett.*, 2011, **11**, 2119.

4 K. Sivula, R. Zboril, F. Le Formal, R. Robert, A. Weidenkaff, J. Tucek, J. Frydrych and M. Gratzel, *J. Am. Chem. Soc.*, 2010, **132**, 7436.

5 T. K. Townsend, E. M. Sabio, N. D. Browning and F. E. Osterloh, *Energy Environ. Sci*., 2011, **4**, 4270.

6 N. Beermann, L. Vayssieres, S. E. Lindquist and A. Hagfeldt, *J. Electrochem. Soc*., 2000, **147**, 2456.

7 Y. S. Hu, A. Kleiman-Shwarsctein, A. J. Forman, D. Hazen, J. N. Park and E. W. McFarland, *Chem. Mater*., 2008, **20**, 3803.

8 A. S. N. Murthy and K. S. Reddy, *Mater. Res. Bull*., 1984, **19**, 241.

9 B. M. Klahr and T. W. Hamann, *J. Phys. Chem. C*, 2011, **115**, 8393.

10 S. Tilley, M. Cornuz, K. Sivula and M. Gratzel, *Angew. Chem. Int. Ed*., 2010, **49**, 6405.

11 Y. S. Hu, A. Kleiman-Shwarsctein, G. D. Stucky and E. W. McFarland, *Chem. Commun.*, 2009, 2652.

12 T. Hisatomi, F. Le Formal, M. Cornuz, J. Brillet, N. Tetreault, K. Sivula and M. Gratzel, *Energy Environ. Sci*., 2011, **4**, 2512.

13 F. Le Formal, N. Tetreault, M. Cornuz, T. Modehl, M. Gratzel and K. Sivula, *Chem. Sci*. 2011, **2**, 737.

14 R. L. Spray, K. J. McDonald and K.-S. Choi, *J. Phys. Chem. C*, 2011, **115**, 3497.

15 U. Ozgur, Ya. I. Alivov, C. Liu, A. Teke, M. A. Reshchikov, S. Doğan, V. Avrutin, S.-J. Cho and H. Morkoc, *J. Appl. Phys.*, 2005, **98**, 041301.

16 Z. L. Wang, *J. Phys.: Condens. Matter*., 2004, **16**, R829.

17 U. Ozgur, D. Hofstetter and H. Morkoc, *Proceedings of the IEEE*, 2010, **98**, 1255.

18 Z. Fan, X. Wen, S. Yang and J. G. Lu, Appl. Phys. Lett., 2005, 87, 013113.

19 F. Le Formal, M. Gratzel and K. Sivula, *Adv. Funct. Mater*., 2010, **20**, 1099.

20 S. Kumari, A. P. Singh, Sonal; D. Deva, R. Shrivastav, S. Dass and V. R. Satsangi, Int. *J. Hydrog. Energy*, 2010, **35**, 3985.

21 M. L. Zhang, W. J. Luo, Z. S. Li, T. Yu and Z. G. Zou, *Appl. Phys. Lett*., 2010, **97**, 105 (3pp).

22 S. S. Shinde, R. A. Bansode, C. H. Bhosale and K. Y. Rajpure, *J. Semicond.* 2011, **32(1)**, 013001.

23 Y. Q. Li and R. van de Krol, *Chem. Phys. Lett*., 2009, **479**, 86.

24 Y. Q. Liang, C. S. Enache and R. van de Krol, *Int. J. Photoenergy*, 2008, 739864.

25 G. M. Wang, Y. C. Ling, D. A. Wheeler, K. E. N. George, K. Horsley, C. heske, J. Z. Zhang and Y. Li, *Nano Lett*. 2011, **11**, 3503.

26 J. J. H. Pijpers; M. T. Winkler, Y. Surendranath, T. Buonassisi and D. G. Nocera. *PNAS*, 2011, **108**, 10056.

27 R. van de Krol and M. Gratzel (eds.), *Photoelectrochemical Hydrogen Production*, Springer, LLC, 2012, VIII.

28 T. Okumura and C. Kaneshiro. *Electronics and Communications in Japan*, Part 2, 1999, 82(5), 13.